

Dynamical Calculation for Mass and Charge Distributions of Primary Fragments in Strongly Damped Collisions

Junlong Tian, Yubing Li, Pengfei Ma and Di Yuan*

School of Physics and Electrical Engineering, Anyang Normal University, Anyang, 455000, China

Abstract

Mass, charge and mass asymmetry distributions of fission primary fragments produced in strongly damped reactions U+U and Th+Cf have been studied within a microscopic transport model, namely improved molecular dynamical model (ImQMD). We find that the three distributions above mentioned strongly depend on target-projectile combination, incident energy and impact parameters.

Keywords

Superheavy fragments; Strongly damped collision; ImQMD Model; Large mass transfer process; Quasi-fission Process.

1. Introduction

The existence of the “Island of Stability” in the superheavy mass region around atomic number $Z = 114$ and neutron number $N = 184$ has been predicted using the nuclear shell model [1]. In recent 20 years, the progress of experimental research on synthesis of superheavy element (SHE) is remarkable. The production of new superheavy elements are reported at Dubna, RIKEN [1-3], FLNR [2-4] and GSI using fusion reactions [5]. These experiments on the synthesis of superheavy elements (SHE) have been focused on the investigation of this region and seem to support this hypothesis. However, the physicists encountered more and more difficulties during their further experiment by complete fusion reaction mechanism. It was established that the fusion reaction is limited for two reasons. Firstly, the limited by the neutron number of available target-projectile combinations, make further experimental hardly to reach the central area of superheavy “island”. Secondly, the limited of smaller and smaller production cross-section and very narrow width of the excitation function with the increasing of atomic number, make further experimental beyond the ability of present facilities [5]. In this connection, other ways to the production of superheavy elements in this region of the “island of stability” should be searched for. An alternative pathway to the superheavy elements is strongly damped collisions since it overcome the limit of neutron number of target-projectile combinations can be produce very neutron-rich superheavy nuclei. What is strongly damped collision? This process is shown by the lower branch of Figure 1 from Ref. [1] with their characteristic time scales in units of 10^{-21} s. The upper branch illustrates complete fusion. The lower branch shows the two interacting nuclei stick together for some time, about 10^{-21} s magnitude, forming a composite system, and then most of events the composite system separates again into two nuclei roughly identical with the interacting nuclei in entrance channel. In this contact time, the kinetic energy of the projectile can be completely transformed into internal excitation and into rotation, and hence the process is called strongly damped collision. During such a reaction a substantial number of protons and neutrons can be transferred between the interacting nuclei. But we find that a very few events the composite system separates into two nuclei, a big one and a small one, in simulation reactions by the improved quantum molecular dynamics (ImQMD) model. This asymmetry fission may be lead to produce of SHE. These fragments are called primary fragments, thereinto, the fragments with atomic number $Z \geq 114$ are called

superheavy fragments (SHFs). When superheavy fragments are formed in nuclear reactions they carry a certain excitation energy and rotate with a certain angular momentum. Both these effects decrease the effective fission barrier. So, most of the superheavy fragments formed in damped collisions will decay by fission, but a small fraction originating with very low excitation may survive [6]. Encouraged by this theory, we are going to renewedly consider such a reaction mechanism to produce SHFs with the optimal incident energy by using the ImQMD model.

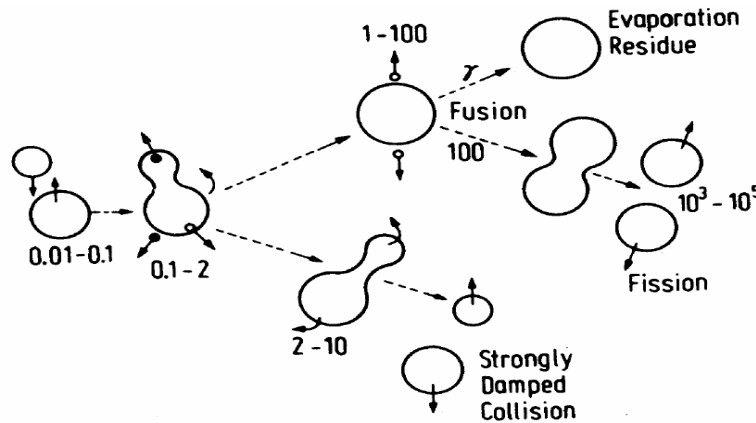


Figure 1. Schematic picture of superheavy nucleus formation (in units of $10^{-21}s$).

2. The ImQMD model

The quantum molecular dynamics (QMD) model being successfully used in intermediate-energy heavy-ion collisions has been successfully extended to heavy-ion collisions at energies near barrier by making serious improvements [7,8]. It is called the "improved quantum molecular dynamics (ImQMD)". In the ImQMD model, the same as in the original QMD model [9,10], each nucleon is represented by a Gaussian wave packet,

$$\phi_i^{\mathbf{k}}(\mathbf{r}) = \frac{1}{(2\pi L)^{3/4}} \exp\left[-\frac{(\mathbf{r} - \mathbf{r}_i)^2}{4L} + \frac{i\mathbf{p}_i \cdot \mathbf{r}}{\hbar}\right], \tag{1}$$

Where \mathbf{r}_i and \mathbf{p}_i are the centers of the i -th wave packet in the coordinate and momentum space, respectively. σ_r represents the spatial spread of the wave packet. The total N -body wave function is assumed to be the direct product of these coherent states. Through a Wigner transformation, the one-body phase space distribution function for N -distinguishable particles is given by

$$\begin{aligned} f_i(\bar{\mathbf{r}}, \bar{\mathbf{p}}) &= \frac{1}{(2\pi\hbar)^3} \int \exp\left(\frac{-i\bar{\mathbf{r}}_{12} \cdot \bar{\mathbf{p}}_{12}}{\hbar}\right) \phi_i^* \phi_i d\bar{\mathbf{r}}_{12} \\ &= \frac{1}{(\pi\hbar)^3} \exp\left(\frac{-(\bar{\mathbf{r}} - \bar{\mathbf{r}}_i)^2}{2L}\right) \exp\left(\frac{-(\bar{\mathbf{p}} - \bar{\mathbf{p}}_i)^2 \cdot 2L}{\hbar^2}\right). \end{aligned} \tag{2}$$

For identical fermions, the effects of the Pauli principle are discussed in Ref. [11]. The approximative treatment of antisymmetrization is adopted in the ImQMD model by means of the phase space occupation constraint method [12]. The density and momentum distribution of a system read

$$\rho(\vec{r}) = \int f(\vec{r}, \vec{p}) d\vec{p} = \frac{1}{(2\pi\sigma_r^2)^{3/2}} \sum_i \exp\left(-\frac{(\vec{r} - \vec{r}_i)^2}{2\sigma_r^2}\right) \quad (3)$$

$$g(\vec{p}) = \int f(\vec{r}, \vec{p}) d\vec{r} = \frac{1}{(2\pi\sigma_p^2)^{3/2}} \sum_i \exp\left(-\frac{(\vec{p} - \vec{p}_i)^2}{2\sigma_p^2}\right) \quad (4)$$

respectively, where the sum runs over all particles in the system. where σ_r and σ_p are the widths of wave packets in coordinate and momentum space, respectively, and they satisfy the minimum uncertainty relation

$$\sigma_r \cdot \sigma_p = 1/2. \quad (5)$$

The propagation of nucleons under the self-consistently generated mean field is governed by Hamiltonian equations of motion:

$$\dot{\vec{r}}_i = \frac{\partial H}{\partial \vec{p}_i}, \quad \dot{\vec{p}}_i = -\frac{\partial H}{\partial \vec{r}_i}. \quad (6)$$

The Hamiltonian H consists of the kinetic energy and effective interaction potential energy, i.e.,

$$H = T + U, \quad (7)$$

$$T = \sum_i \frac{P_i^2}{2m} \quad (8)$$

The effective interaction potential energy includes the nuclear local interaction potential energy and Coulomb interaction potential energy,

$$U = U_{loc} + U_{Coul}. \quad (9)$$

U_{loc} is obtained from the integration of the nuclear local interaction potential energy density functional. The nuclear local interaction potential energy density functional $V_{loc}(\rho(r))$ is taken as the same as that in Ref. [8], which reads

$$V_{loc} = \frac{\alpha}{2} \frac{\rho^2}{\rho_0} + \frac{\beta}{\gamma+1} \frac{\rho^{\gamma+1}}{\rho_0^\gamma} + \frac{g_0}{2\rho_0} (\nabla\rho)^2 + g_t \frac{\rho^{\eta+1}}{\rho_0^\eta} + \frac{C_s}{2\rho_0} (\rho^2 - \kappa_s (\nabla\rho)^2) \delta^2. \quad (10)$$

Here ρ and δ are the nucleon density and the isospin asymmetry. By integrating V_{loc} , we obtain the local interaction potential energy

$$U_{loc} = \frac{\alpha}{2} \sum_{i,j \neq i} \frac{\rho_{ij}}{\rho_0} + \frac{\beta}{\gamma+1} \sum_{i,j \neq i} \left(\frac{\rho_{ij}}{\rho_0} \right)^\gamma + \frac{g_0}{2} \sum_{i,j \neq i} f_{s(ij)} \frac{\rho_{ij}}{\rho_0} + g_\tau \left(\frac{\rho_{ij}}{\rho_0} \right)^\eta + \frac{C_s}{2} \sum_{i,j \neq i} t_{iz} t_{jz} \frac{\rho_{ij}}{\rho_0} (1 - \kappa_s f_{s(ij)}), \quad (11)$$

$$\rho_{ij} = \frac{1}{(4\pi\sigma_r^2)^{3/2}} \exp\left(-\frac{(r_i^{\mathbf{k}} - r_j^{\mathbf{k}})^2}{4\sigma_r^2}\right) \quad (12)$$

$$f_{s(ij)} = \frac{3}{2\sigma_r^2} - \left(\frac{r_{ij}}{2\sigma_r^2} \right)^2 \quad (13)$$

and $t_{iz} = 1$ and -1 for proton and neutron, respectively.

The Coulomb energy is written as the sum of the direct and the exchange contribution, the latter being taken into account in the Slater approximation

$$U_{coul} = \frac{1}{2} \int \rho_P(\mathbf{r}^{\mathbf{k}}) \frac{e^2}{|\mathbf{r}^{\mathbf{k}} - \mathbf{r}^{\mathbf{k}_1}|} \rho_P(\mathbf{r}^{\mathbf{k}_1}) d\mathbf{r}^{\mathbf{k}} d\mathbf{r}^{\mathbf{k}_1} - e^2 \frac{3}{4} \left(\frac{3}{\pi} \right)^{1/3} \int \rho_P^{4/3} dR, \quad (14)$$

where the parameters used are the same as in Ref. [13] (see Table 1).

A proper initial condition is of crucial importance for application of the ImQMD model to low-energy heavy-ion reactions. In this work, the procedure of making initial nuclei of projectile and target is similar to that in Refs. [7,8,13]. The binding energies for ^{238}U , ^{232}Th , and ^{250}Cf are required to be 7.57 ± 0.05 , 7.62 ± 0.05 , and 7.48 ± 0.05 MeV/nucleon, and the root-mean-square radii are required to be 7.36 ± 0.2 , 7.34 ± 0.2 , and 7.53 ± 0.2 fm, respectively. The stability of the pre-prepared initial nuclei is well checked. It is tested whether those prepared nuclei satisfy the requirements that their binding energies and rms charge radii maintain the proper values required by the properties of initial nuclei with a very small fluctuation and that they evolve stably without spurious emission within 3000 fm/c. Only those that satisfy the requirements will be taken as the "initial nuclei" and stored for usage in reaction simulations. Before extending the model to the study of low-energy reactions of transactinide nuclei, we first apply the model to low-energy reactions of heavy nuclei. Since we are now mainly interested in the average behavior of the composite systems, the initial deformation of the projectile and target nuclei is not considered in this work for simplicity.

Table 1. Model parameters

Para	α MeV	β MeV	γ	g_τ MeV	g_0 MeVfm ²	η	C_s MeV	κ_s fm ²	ρ_0 fm ⁻³
IQ2	-356	303	7/6	12.5	7	2/3	32	0.08	0.165

3. Results

3.1. The Energy-dependence of Production Probability of SHFs

In the present work, we have studied reactions of $^{238}\text{U}+^{238}\text{U}$ and $^{232}\text{Th}+^{250}\text{Cf}$ at the energy range of $E_{c.m.} = 800\text{-}2000$ MeV by the ImQMD model. We will concentrate on the energy-dependence of the probability of producing SHFs with $Z \geq 114$, the impact parameter is taken to be 1 fm and the initial center-of-mass distance of projectile and target is 50 fm in simulation process. The simulation events are taken to be 1000 for every energy point and impact parameter and for

saving CPU time the simulation procedure is carried out as follows: for each event, the simulation will be terminated if there is no fission fragment with $Z \geq 114$, otherwise the simulation will be continued until $t = 6000 \text{ fm/c}$.

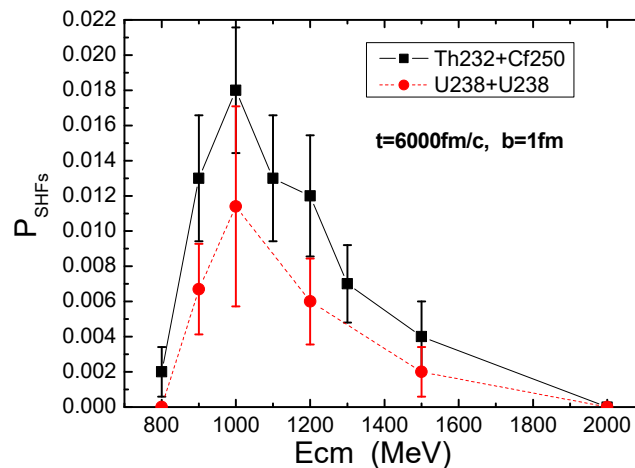


Figure 2. The incident energy dependence of the production probability of superheavy fragments with $Z \geq 114$ in reaction $^{238}\text{U}+^{238}\text{U}$ and $^{232}\text{Th}+^{250}\text{Cf}$ with impact parameter $b=1\text{fm}$. Error bars indicate statistical deviations.

Figure 2 shows the energy dependence of the probability of producing superheavy fragments for two reactions of $^{238}\text{U}+^{238}\text{U}$ and $^{232}\text{Th}+^{250}\text{Cf}$ at the energy range of $E_{c.m.} = 800\text{-}2000 \text{ MeV}$. It shows us that among these two reactions, the yield of SHFs with $Z \geq 114$ produced in $^{232}\text{Th}+^{250}\text{Cf}$ is the higher than that produced in $^{238}\text{U}+^{238}\text{U}$. It means that the strongly damped reaction with asymmetry than symmetry reaction systems could be very beneficial for producing superheavy nuclei. The very pronounced feature of the figure is that it is narrowly peaked in the energy dependence of the production probability of SHFs and the location of the peak is at about $E_{c.m.} = 1000 \text{ MeV}$ for the $^{232}\text{Th}+^{250}\text{Cf}$ and $^{238}\text{U}+^{238}\text{U}$. Although the precise location of peak energy may not be very definite in this primary calculation, such behavior of the energy dependence of the probability of superheavy fragments with $Z \geq 114$ should be correct. The narrow peak means that it is crucial to select the correct incident energy in order to search superheavy elements experimentally by using the approach of the strongly damped massive reactions. In our calculation, when the incident center-of-mass energy $E_{c.m.} = 1000 \text{ MeV}$, the collision is more violent and there happens the transfer of much more nucleons though the mass loss from the system is also large. We also notice that the experiments about $^{232}\text{Th}+^{250}\text{Cf}$ and $^{238}\text{U}+^{238}\text{U}$ had been done in the 1970s and the early of 1980s [14-17]. In these experiments thick targets have been used, which means that the experimental data were, integrated over the energy in the region of about $E_{c.m.} = 730\text{-}893 \text{ MeV}$ and $E_{c.m.} = 757\text{-}899 \text{ MeV}$, while the coulomb barriers were 730 MeV and 757 MeV for reactions $^{238}\text{U}+^{238}\text{U}$ and $^{232}\text{Th}+^{250}\text{Cf}$, respectively. So, one could find that the incident energy at that time is very close to the coulomb barrier and lower than the peak energy for the reaction of $^{238}\text{U}+^{238}\text{U}$. The production probability of SHFs corresponding to the energies used in [14-17] is much lower than that at the peak energy.

3.2. Mass and Charge Distributions of Primary Fission Fragments of $^{238}\text{U} + ^{238}\text{U}$

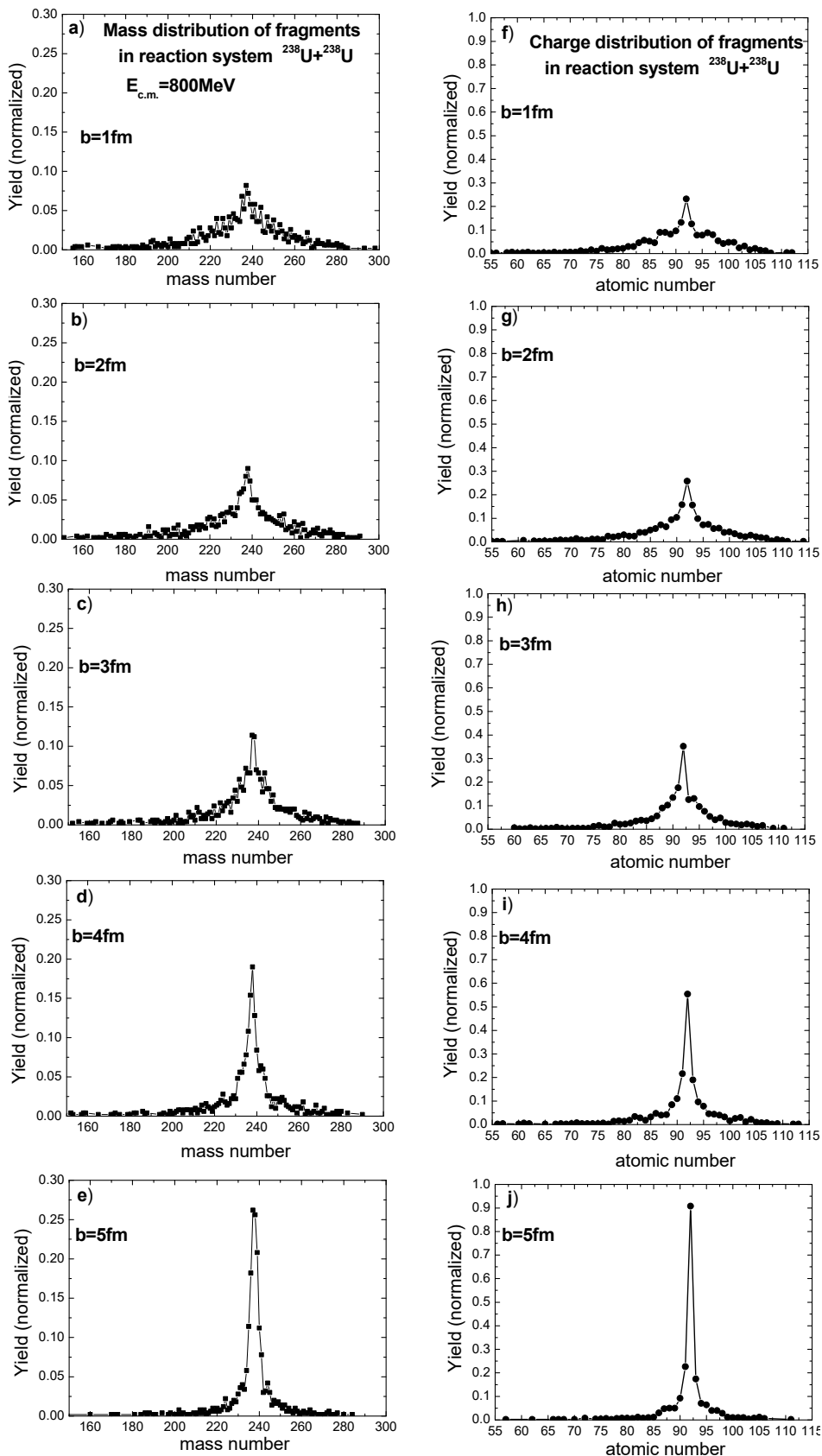


Figure 3. Mass [(a)-(e)] and charge [(f)-(j)] distributions of the primary fission fragments in the $^{238}\text{U} + ^{238}\text{U}$ reaction at 800 MeV center-of-mass energy with impact parameters $b = 1-5$ fm

First we analyze the mass and charge distributions of the $^{238}\text{U}+^{238}\text{U}$ reaction at incident center-of-mass energy $E_{c.m.} = 800$ MeV with impact parameters $b = 1-5$ fm, the large mass transfer process is very little in this incident energy region, while mainly reaction process is quasi-fission or a few nucleons transferred reaction and investigate how the impact parameters affects the Mass and Charge distribution. Figure 3 shows the mass distributions (a)-(e) and charge distributions (f)-(j) of the primary fission fragments in the reaction $^{238}\text{U}+^{238}\text{U}$. From subfigure (a)-(e) or (f)-(j), one can see that the peak (238 in mass distributions or 92 in the charge distributions) become higher and higher, it means that the number transferred nucleons become less and less with the increasing of impact parameter $b = 1$ fm to 5 fm. This is to say, the large mass transfer process is less and less with the increasing of impact parameter, while the most of reaction events is quasi-fission or a few nucleons transferred reaction since projectile and target keep themselves personality. This may be because of the increasing of impact parameter the torque become larger and larger, and then make the effective coulomb barrier increase. Compare (a) with (f), we find the peak 238 in mass distributions were lower than that 92 in charge distributions, this is to say, the neutron number transferred is larger than the proton number in strongly damped reaction U+U with incident energy $E_{c.m.} = 800$ MeV.

Large charge and mass transfer was found due to the asymmetric fission process leading to formation of the superheavy fragments. For the first time a common mass and charge asymmetry degree of freedom are defined in fission channels (quasi-fission) with formation of fission fragments. The mass asymmetry $\eta = (A_1 - A_2) / (A_1 + A_2)$ of the primary fission fragments in the ImQMD calculation. Here A_1 and A_2 are the largest and the second largest fragment mass when the fission occurs, respectively, and the largest fragment mass is larger than or equal to the initial target mass number.

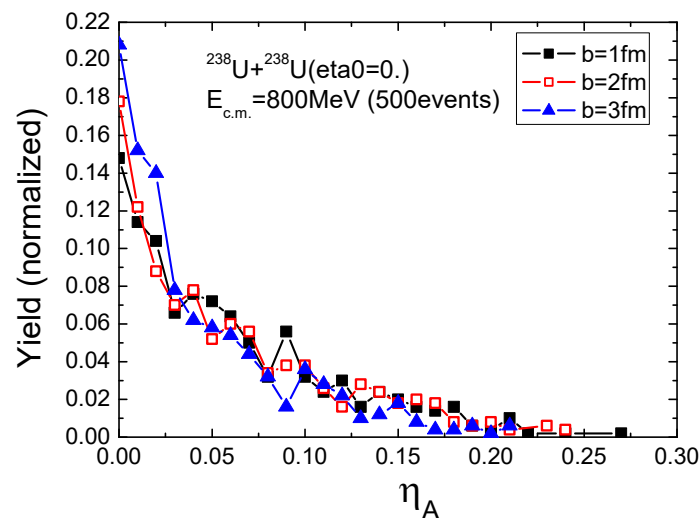


Figure 4. The mass asymmetry distributions of the SHFs in the reaction $^{238}\text{U}+^{238}\text{U}$ at the incident energy $E_{c.m.} = 800$ MeV with impact parameters $b = 1-3$ fm.

The final fragments mass asymmetry degree of freedom is a better physical quantity to reflect charge and mass transfer in strongly damped collisions. Figure 4 shows the mass asymmetry distributions of the primary fission fragments in the reaction $^{238}\text{U}+^{238}\text{U}$ at the incident energy $E_{c.m.} = 800$ MeV with impact parameters $b = 1-3$ fm. In Figure 4, the largest value of mass-asymmetry is decreasing, from 0.27 with $b = 1$ fm to 0.24 with $b = 2$ fm, and then to 0.21 with $b = 3$ fm; while peak of yield in the mass asymmetry distributions is increasing with the impact parameter enhancement from 0.15 ($b = 1$ fm) to 0.18 ($b = 2$ fm), and then 0.21 ($b = 3$ fm). It also means that transferred nucleons events become less and less with the increasing of impact parameter $b = 1$ fm to 3 fm. This is to say, the large mass transfer process is less and less with

the increasing of impact parameter, while the most of reaction events is quasi-fission or a few nucleons transferred reaction.

3.3. Mass and Charge Distributions of Primary Fission Fragments of $^{232}\text{Th} + ^{250}\text{Cf}$

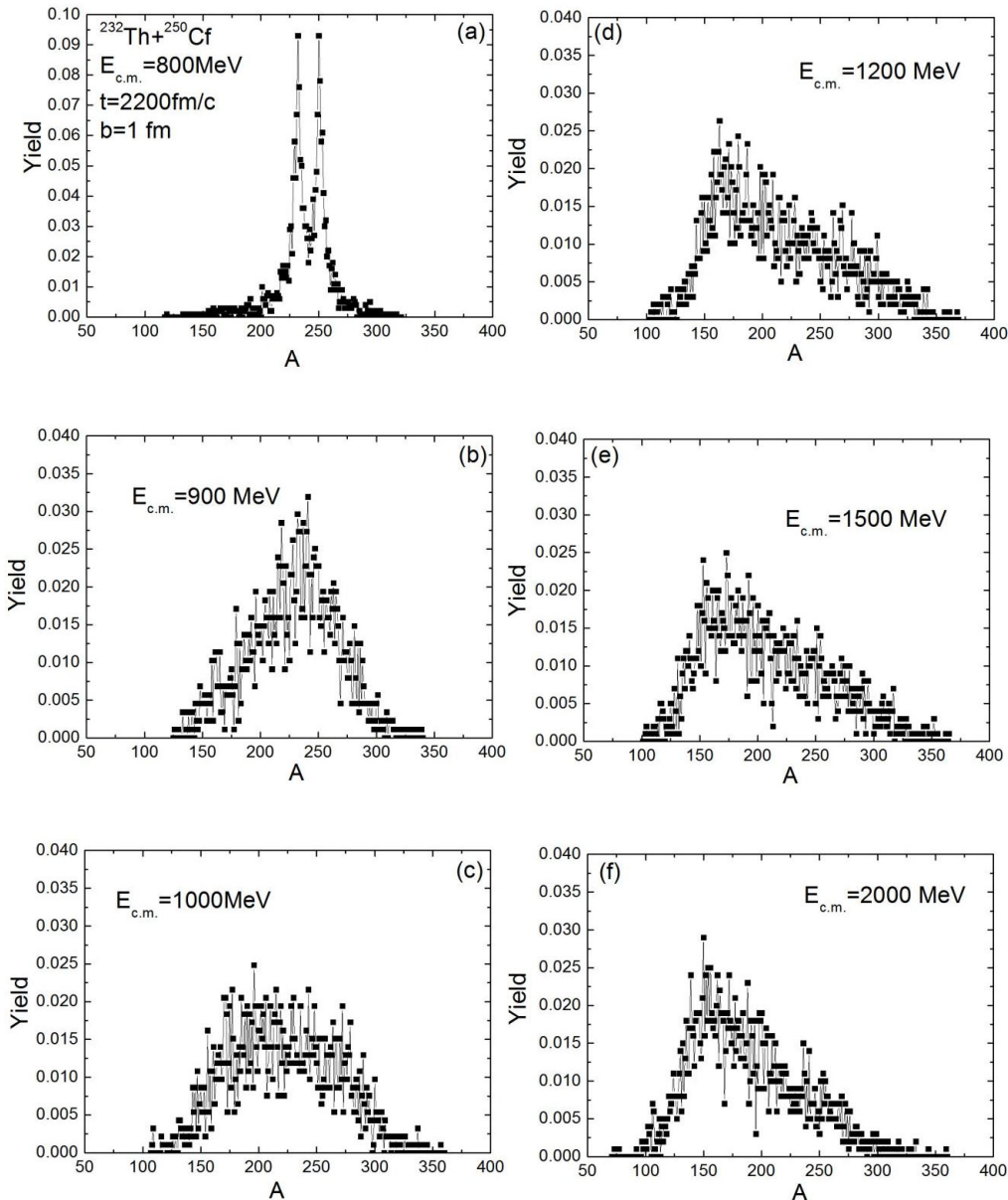


Figure 5. Mass distributions of the primary fission fragments in the reaction $^{232}\text{Th} + ^{250}\text{Cf}$ at the incident energy $E_{c.m.} = 800\text{-}2000 \text{ MeV}$ with impact parameters $b = 1 \text{ fm}$.

For $^{232}\text{Th} + ^{250}\text{Cf}$ reaction the situation changes compare with $^{238}\text{U} + ^{238}\text{U}$ reaction and investigate how the the incident energies affects the Mass and Charge distributions. Figure 5 shows the mass distributions [(a)-(f)] of the primary fission fragments in the reaction $^{232}\text{Th} + ^{250}\text{Cf}$ at the incident energy $E_{c.m.} = 800\text{-}2000 \text{ MeV}$ with impact parameters $b=1 \text{ fm}$. From subfigure 5 (a), one can see that there are two peaks in mass distributions of primary fission fragments in reaction $^{232}\text{Th} + ^{250}\text{Cf}$ with incident energy $E_{c.m.} = 800 \text{ MeV}$. The two peaks are the initial mass of projectile 232 and target 250 nuclei, respectively. it looks like a rabbit ears. The largest fragment mass is not more than 300. But the situation changes with the increasing of incident energy, when $E_{c.m.} = 900 \text{ MeV}$, the mass distributions in subfigure 5 (b) of primary fission fragments has a marked difference compare to that when $E_{c.m.}=800\text{MeV}$ in Figure 5 (a), there

is no peak in mass distribution, but wide region. The largest fragment mass reaches 320. But the situation further change with the increasing of incident energy, when $E_{c.m.}=1000\text{MeV}$, the mass distributions in subfigure 5 (c) of primary fission fragments has a flat roof from 160 to 280. This means that the production probability of fragments is almost equal in mass region 160 - 280. The largest fragment mass is also about 320. From $E_{c.m.} = 1100\text{-}2000\text{ MeV}$, the mass distributions of primary fission fragments become higher at 160 than that at 280. The mass distributions have little difference in Figure 5(d)-(f). The largest fragment mass is decreasing from more than 320 to less 300 with incident energy increasing from $E_{c.m.} = 1100\text{ MeV}$ to 2000 MeV. There are largest fragment over 320 at incident center-of-mass energy equal 1100 MeV. This may be because of the increasing of incident energy, the excitation energy of composite systems become larger and larger and easy to fragmentate. Figure 6 shows the charge distributions (a)-(f) and of the primary fission fragments in the reaction $^{232}\text{Th} + ^{250}\text{Cf}$ at the incident energy $E_{c.m.} = 800\text{-}2000\text{ MeV}$ with impact parameters $b = 1\text{ fm}$ according to that in Figure 5. The situation is the same as what we observed in Figure 5

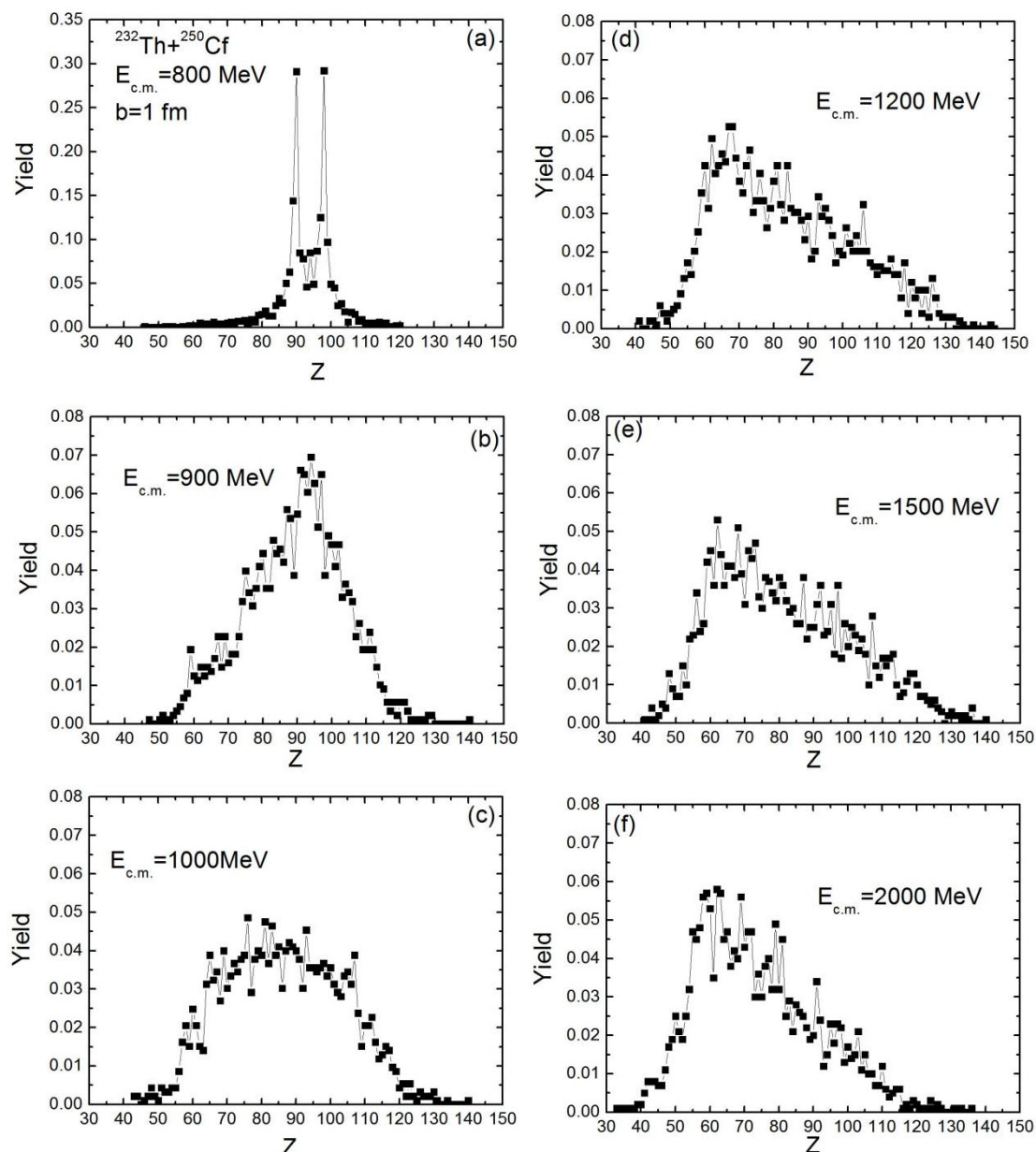


Figure 6. Charge distributions of the primary fission fragments in the reaction $^{232}\text{Th} + ^{250}\text{Cf}$ at the incident energy $E_{c.m.} = 800\text{-}2000\text{ MeV}$ with impact parameters $b = 1\text{ fm}$.

In Figure 7, the largest value of mass-asymmetry η is reaching 0.235 when impact parameter $b = 1$ fm, while the largest value of mass-asymmetry almost equal is 0.225 when $b = 2-4$ fm, the minimum value is 0.175 with $b = 5$ fm; while peak of yield in the mass asymmetry distributions is increasing with the impact parameter enhancement from 0.21 ($b = 1$ fm) to 0.45 ($b = 5$ fm). It means that transferred nucleons events become less and less with the increasing of impact parameter $b = 1$ fm to 5 fm. This is to say, the large mass transfer process is less and less with the increasing of impact parameter, while the most of reaction events is quasi-fission or a few nucleons transferred reaction.

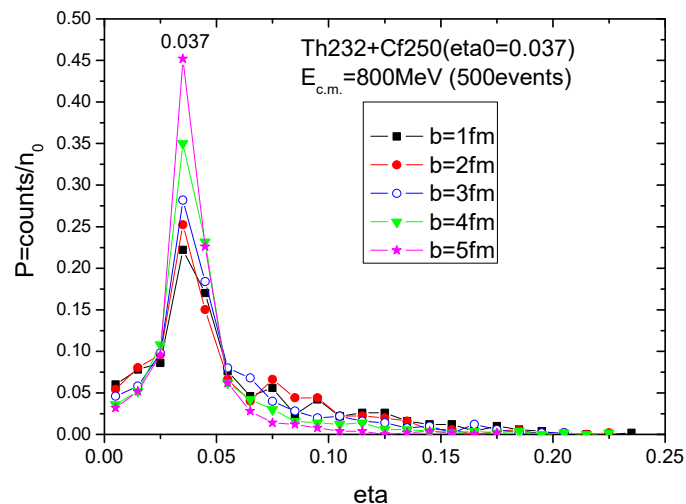


Figure 7. The mass asymmetry distributions of the primary fission fragments in the asymmetry reaction $^{232}\text{Th} + ^{250}\text{Cf}$ at the incident energy $E_{c.m.} = 800$ MeV with impact parameters $b = 1-5$ fm.

4. Summary and Conclusion

The strongly damped collisions U+U and Th+Cf were studied by simulation using the ImQMD model. We calculated the production probability of SHFs with $Z \geq 114$ and found it strongly depends on the incident energy, and found that the production probability of SHFs for asymmetric reaction Th+Cf is much higher than that for symmetric reaction U+U. The mass, charge distributions and mass asymmetry and charge asymmetry distributions had also been discussed, and drew a conclusion that the distributions above mentioned strongly depend on target-projectile combinations, incident energy and impact parameter. We also found that the production of SHFs seems to be quite possible due to a large mass and charge rearrangement in the asymmetry fission process of composite system created by projectile and target. In the next step, we should consider the dynamical deformation of fragments for the production process of SHFs. In the superheavy mass region, the degree of freedom of the fragment deformation is very important because many trajectories move in the direction of the large deformation of the fragment in the present two-center shell model shape parameterization. For the future study, we also should investigate the production probability of SHFs with $Z \geq 114$ evolution with the time and further give the curvature of the production probability. The excitation energy, angular momentum, survival probability of SHFs with $Z \geq 114$, the cross section of residue superheavy nuclei and the lifetime of composite system created by projectile and target should be estimated.

Acknowledgments

This work was supported by the Special Program for Basic Research of the key scientific research projects in universities of Henan Province (Grant No. 21zx015), and the Innovation Foundation for Students of Anyang Normal University (Grant Nos. 202110479024, 202110479092).

References

- [1] W.D. Myers, W.J. Swiatecki, Nucl. Phys. 81 (1966) 1;
- [2] Yu.Ts. Oganessian, et al., Nature 400 (1999) 242;
- [3] Yu.Ts. Oganessian, et al., Phys. Rev. C 63 (2001) 011301(R).
- [4] Yu.Ts. Oganessian, et al., Phys. Rev. C 69 (2004) 021601(R).
- [5] S. Hofmann, G. Munzenberg, Rev. Mod. Phys. 72 (2000) 733;
- [6] L. G. Moretto, Nucl. Phys. A 180, 337(1972)
- [7] N. Wang; Z.X. Li, and X. Z. Wu., Phys. Rev. C,65, (2002) 064608.
- [8] N. Wang; Z.X. Li, and X. Z. Wu and J.L. Tian, Phys. Rev. C, 69, (2004) 034608.
- [9] C. Hartnack, Z.X. Li, L. Neise, et al. Nucl.Phys.A 495, 495, (1989) 303-309.
- [10] J. Aichelin, J. Phys. Rep. 202, (1991) 233-360.
- [11] H. Feldmeier, and J. Schnack, Rev. Mod. Phys. 72, (2000) 655-688.
- [12] M. Papa, T. Maruyama and A. Bonasera, . Phys. Rev. C, 64, (2001) 024612.
- [13] N. Wang, Z.X. Li, X.Z. Wu et al., Mod. Phys. Lett. A, 20, (2005) 2619-2627.
- [14] Gunter Herrmann, Nature (London) 280, 543 (1979).
- [15] H. Gaggeler, N. Trautmann, W. Bruchle et al., Phys. Rev. Lett. 45, 1824 (1980).
- [16] K. D. Hildenbrand, H. Freiesleben, F. Pühlhofer et al., Phys. Rev. Lett. 39, 1065 (1977).
- [17] M. Schadel, W. Bruchle, H. Gaggeler et al., Phys. Rev. Lett. 48, 852 (1982).